This is the accepted manuscript made available via CHORUS. The article has been published as:

Breaking and trapping Cooper pairs by Rydberg-molecule spectroscopy in atomic Fermi superfluids

Chih-Chun Chien, S. I. Mistakidis, and H. R. Sadeghpour

Phys. Rev. A **110**, L051303 — Published 18 November 2024

DOI: 10.1103/PhysRevA.110.L051303

Breaking and trapping Cooper pairs by Rydberg-molecule spectroscopy in atomic Fermi superfluids

Chih-Chun Chien,[1,2,*] S. I. Mistakidis,[1,3] and H. R. Sadeghpour[1]

[1] *ITAMP, Center for Astrophysics | Harvard & Smithsonian, Cambridge, USA*
[2] *Department of Physics, University of California, Merced, CA, USA*
[3] *Department of Physics, Missouri University of Science and Technology, Rolla, MO, USA*

We propose a spectroscopic probe of the breaking and localization of Cooper pairs in an atomic Fermi superfluid interacting with a Rydberg impurity. This is achieved by monitoring the formation of diatomic and triatomic ultralong-range molecular species in the superfluid across the Bardeen–Cooper–Schrieffer (BCS)-Bose Einstein condensation (BEC) crossover. The triatomic Rydberg molecule in the BEC regime heralds the trapping of a tightly-bound Cooper pair, reminiscent of pion capture in nuclear matter, while the breaking of a Cooper pair on the BCS side by a diatomic Rydberg molecule is evocative of binary-star tidal disruption by a black hole. Spectroscopy of the Fermi superfluid and Rydberg molecules allows for an estimation of the Cooper-pair size while the Rydberg molecule binding energies discern many-body pairing effects.

Rydberg atom-based systems have emerged as leading platforms for demonstrating many-body correlations [1], quantum simulations [2–4], quantum error corrections [5], and quantum optics [6]. When the excited electron scatters from a nearby ground-state atom, under certain conditions, ultralong-range molecular bonds can form [7–9]. Such long-range Rydberg molecules have been realized [10–16]. Interesting aspects of many-body physics, such as the formation of Bose and Fermi polarons, quantum statistics of gases exhibiting bunching and anti-bunching, with Rydberg molecules have also been reported [17–21]. These studies exploit the large energy separations between the vibrational energies and the underlying primitive excitations in a quantum gas.

In a different context, two-component fermions with attractive interactions form Cooper pairs and exhibit the Bardeen-Cooper-Schrieffer (BCS) - Bose-Einstein condensation (BEC) crossover pioneered by the experiments with ultracold Fermi gases [22–24] (see also [25–27]). Here, we show that by creating ultralong-range molecules with a Rydberg impurity in a background sea of Cooper pairs, it is possible to a) break the pairs on the BCS side and b) locally trap a Cooper pair on the BEC side. The former bears analogies with the breaking of a binary-star pair by a tidal disruption event into a black hole [28, 29], while the latter is reminiscent of the capture of pions (quark-antiquark pairs) in hydrogen [30, 31], deuterium [32], and helium [33].

By radio-frequency (rf) spectroscopy of the superfluid pairing gap [34, 35] or Rydberg spectroscopy of the molecular lines [17, 19], one may, in a local spectroscopic manner, probe the reaction of the superfluid to tackle topical problems in condensed matter physics, such as the Cooper-pair size and pairing energies [36].

A typical Rydberg potential is illustrated in Fig. 1 with heteronuclear Rydberg molecules formed in Fermi superfluids. These molecules form (1) in a diatomic bond between the impurity and a fermion from a broken Cooper pair and (2) in a triatomic bond - a Cooper pair in a molecule - with the pair trapped in the Rydberg potential. To our knowledge, the latter type of pair trapping has not previously been discussed, and these molecules are different from the trimer Rydberg molecules emanating from two weakly interacting bosons individually trapped by a bosonic Rydberg atom that have been realized [37] and theoretically studied [38, 39]. This work exploits the interplay between two molecule-formation mechanisms, one between the fermions to bind a Cooper pair and the other among the Rydberg and its neighboring atoms to create a Rydberg molecule. Similar competitions influence the physics of the aforementioned astro and nuclear physics examples.

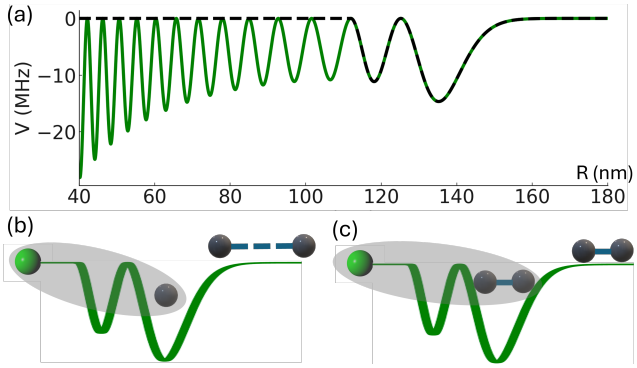


FIG. 1. (a) A typical Rydberg potential (solid line) and the outer double-well approximation (dashed line). The formation of (b) a diatomic Rydberg molecule with a fermion from a broken Cooper pair and (c) a triatomic Rydberg molecule with a Cooper pair. The green (black) spheres represent the Rydberg atoms (fermions in the superfluid). The Cooper pairs are visualized by two black spheres connected by a dashed or solid line. The grey ellipsoids mark the Rydberg molecules.

Leveraging the Bogoliubov-de Gennes (BdG) formalism [40, 41] suitable for studying inhomogeneous effects

* cchien5@ucmerced.edu

in Fermi superfluids, we extract the low-lying bound states of the composite Rydberg-Fermi superfluid system. By increasing the Cooper-pair strength, distinct local reactions of the pairing gap will occur: Breaking (trapping) of a weak (strong) Cooper pair leads to a local suppression (enhancement) of the gap function. We identify the formation of diatomic and triatomic Rydberg molecules along with their binding energies, which are raised by the many-body pairing effect when compared to those in a noninteracting gas. In contrast to previous studies [42] with impurities carrying onsite potentials in Fermi superfluids, the Rydberg potential has its furthest well about hundreds of nanometers away from the core with controllable width and depth, thereby giving rise to rich structures of Rydberg molecules.

Rydberg excitation in a Fermi superfluid.– We consider few Rydberg atoms immersed in a two-component, spin- and mass-balanced Fermi superfluid with contact pairing interactions. Experimentally, this setup can be emulated, for instance, by bosonic ^{87}Rb Rydberg atoms and two hyperfine states of ^{84}Rb or ^{86}Rb for the Fermi superfluid. Relevant experimental progress towards such atomic mixtures can be found in Ref. [43]. However, we emphasize that our results equally hold for other Rydberg atom-Fermi superfluid systems. For simplicity, the Rydberg atoms are assumed to be immobile and noninteracting with each other. A quasi one-dimensional (1D) geometry [44] creating a cigar-shaped cloud similarly to Refs. [24, 45] is considered. It supports the off-diagonal long-range order of the superfluid while freezing out the transverse degrees-of-freedom.

The many-body Hamiltonian of the composite system within the BCS-Leggett theory reads

$$\mathcal{H} = \mathcal{H}_{BCS} + \sum_{\sigma} \int dx V_{Ryd}(x) \psi_{\sigma}^{\dagger}(x) \psi_{\sigma}(x) d^{\dagger} d, \quad (1)$$

where $\mathcal{H}_{BCS} = \int dx \Big[\sum_{\sigma} \psi_{\sigma}^{\dagger}(x) h_{\sigma}(x) \psi_{\sigma}(x) + (\Delta(x) \psi_{\uparrow}^{\dagger}(x) \psi_{\downarrow}^{\dagger}(x) + h.c.) \Big]$ [25, 46]. The fermion operator acting on the $\sigma = \uparrow, \downarrow$ component of mass m is ψ_{σ}, and $h_{\sigma}(x) = -\frac{\hbar^2}{2m}\nabla^2 + V_{ext}(x) - \mu_{\sigma}$ denotes the single-particle Hamiltonian with $V_{ext}(x)$ summarizing the total external confinement. The order parameter of the s-wave Fermi superfluid is the gap function

$$\Delta(x) = -U \langle \psi_{\downarrow}(x) \psi_{\uparrow}(x) \rangle. \quad (2)$$

The effective coupling $U < 0$ is related to the 1D scattering length a_{1D} [47] via $U = -\frac{2\hbar^2}{m a_{1D}}$, tunable by Feshbach resonance [25], and $\langle \dots \rangle$ designates the ground-state expectation value at $T = 0$. The BCS-BEC crossover occurs when the chemical potential (here $\mu_{\uparrow} = \mu_{\downarrow} \equiv \mu$) crosses zero [27] where the minimum of the quasiparticle-spectrum shifts to zero momentum.

Importantly, the second contribution in Eq. (1) models the Rydberg atom - fermion interaction [20], with d ($d^{\dagger}$) being the annihilation (creation) operator of a Rydberg atom. The ultralong-range Born-Oppenheimer potential between a Rydberg atom and a ground-state fermionic atom is given by $V_{Ryd}(x) = \frac{2\pi\hbar^2 a_e}{m_e} |\psi_e(x)|^2$ [7]. Here, a_e denotes the scattering length between the Rydberg electron with mass m_e and a fermionic atom, and x measures the distance from the Rydberg impurity to the fermionic atom. The Rydberg electron wave function, $\psi_e(x)$, is calculated with effective valence potentials [48]. In the vicinity of a Rydberg atom, we replace $d^{\dagger}d$ by $\langle d^{\dagger}d \rangle = 1$ and hence $V_{Ryd}(x)$ acts as an effective potential for the Fermi superfluid. In what follows, the localized Rydberg potential will be implicitly combined with $V_{ext}(x)$ in h_{σ}. Moreover, the Rydberg potential is approximated by the double-well form shown in Fig. 1(a) since the outer two wells represent the two largest lobes of the Rydberg electron wave function of interest (see Ref. [49] for more information), and therefore have the largest Frank-Condon factor for excitation. The Fermi energy $E_f = \hbar^2 k_f^2/(2m)$ and wavevector $k_f = \pi n/2$, of a noninteracting 1D two-component Fermi gas with the same total particle number $N = \int n(x) dx$ as the superfluid serve as the energy and inverse-length units. For example, $g = -U k_f / E_f$ is the dimensionless pairing strength. Here, mean-field theory is used to describe ground-state properties of the quasi-1D system. If critical behavior is encountered, more sophisticated theories may be consulted [27].

BdG formalism. – To reveal the impact of the Rydberg atoms on the Fermi superfluid, we inspect the composite system as the superfluid undergoes the BCS-BEC crossover. Specifically, $\mathcal{H}$ can be diagonalized by the BdG transformation [41, 50]: $\psi_{\uparrow,\downarrow}(x) = \sum_{\tilde{n}} [u_{\uparrow,\downarrow}^{\tilde{n}1,2}(x) \gamma_{\tilde{n}1,2} \mp v_{\uparrow,\downarrow}^{\tilde{n}2,1*}(x) \gamma_{\tilde{n}2,1}^{\dagger}]$. The quasiparticle wave functions $u_{\sigma}^{\tilde{n}j}$ and $v_{\sigma}^{\tilde{n}j}$ with $j = 1, 2$ are to be determined, and they satisfy $\int dx (|u_{\sigma}^{\tilde{n}j}|^2 + |v_{\sigma}^{\tilde{n}j}|^2) = 1$. The BdG equation for the composite system considered here can be block-diagonalized into [41]

$$\begin{pmatrix} h_{\uparrow}(x) & \Delta(x) \\ \Delta^*(x) & -h_{\downarrow}^*(x) \end{pmatrix} \begin{pmatrix} u_{\uparrow}^{\tilde{n}j}(x) \\ v_{\downarrow}^{\tilde{n}j}(x) \end{pmatrix} = E_{\tilde{n}j} \begin{pmatrix} u_{\uparrow}^{\tilde{n}j}(x) \\ v_{\downarrow}^{\tilde{n}j}(x) \end{pmatrix}. \quad (3)$$

Moreover, the BdG equation has a discrete symmetry connecting the positive and negative energy states, so we drop the indices $1, 2$ and $\uparrow, \downarrow$ from the quasi-particle wave functions. For the ground state, the gap function Eq. (2) then becomes $\Delta(x) = -U \sum_{\tilde{n}}{}' u_{\uparrow}^{\tilde{n}}(x) v_{\downarrow}^{\tilde{n}*}(x)$ and the total fermion density $n(x) = \sum_{\sigma} n_{\sigma}(x) = 2 \sum_{\tilde{n}}{}' |v_{\tilde{n}}(x)|^2$ with $n_{\sigma}(x) = \langle \psi_{\sigma}^{\dagger}(x) \psi_{\sigma}(x) \rangle$. Here $\sum_{\tilde{n}}{}'$ denotes summation over the positive-energy states. We discretize the space and implement an iterative method [41, 51] to solve the BdG equation (see SM [52] for details).

Spectroscopic signatures of pair breaking and pair trapping.– To account for the impenetrable core of the Rydberg atom, the system is embedded in a 1D box of size L with the Rydberg atom at $x = 0$ and appropriately adjusting the relevant energy and length scales, see also SM [52]. The gap function and density of a representative BCS (BEC) Fermi superfluid with $\mu > 0$ ($\mu < 0$)

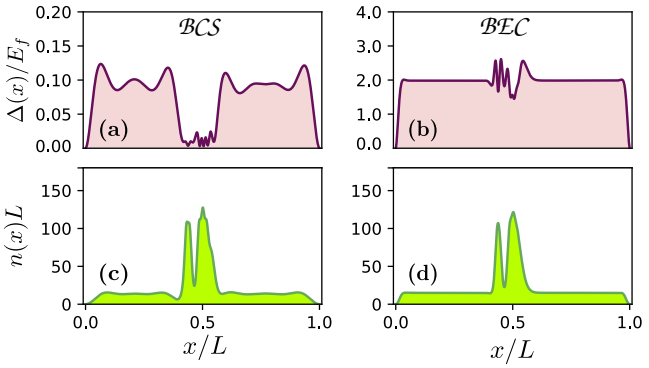


FIG. 2. Gap function Δ (top panels) and density (bottom panels) of a Fermi superfluid in the BCS regime with $g = 0.7$, $\mu = 0.20E_f$ (left panels) and the BEC regime where $g = 3.6$ and $\mu = -0.46E_f$ (right panels) under the same Rydberg potential. Reduced (enhanced) undulations of $\Delta(x)$ near the wells of the Rydberg potential are evident in the BCS (BEC) regime.

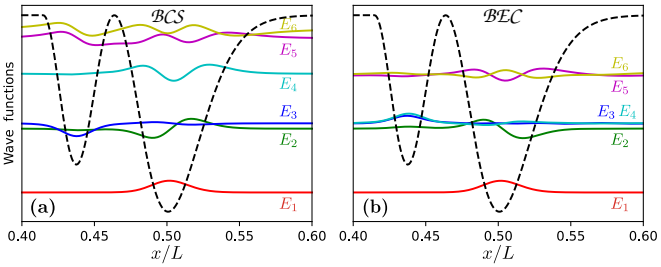


FIG. 3. Bound vibrational wave functions $v_n(x)$ of the Rydberg potential (dashed lines) depicted in Fig. 1 offset according to their energies E_n. The Fermi superfluid is in the (a) BCS regime with $g = 0.7$ and $\mu = 0.20E_f$ and (b) BEC regime with $g = 3.6$ and $\mu = -0.46E_f$. On the BEC side, there are two sets of nearly degenerate vibrational states localized respectively in the inner and outer wells, heralding the formation of triatomic heteronuclear Rydberg molecules.

subjected to the Rydberg potential are depicted in the left (right) panels of Fig. 2. While the density profiles on both BCS and BEC sides show peaks evidencing the bound states due to the attractive Rydberg potential, the most prominent contrast is the enhancement (suppression) of the gap function around the minima of the Rydberg potential in the BEC (BCS) regime. The decoupling of the gap function and density of a Fermi superfluid on the BCS side has also been discussed in vortex structures [53, 54]. The oscillatory boundary effects on the BCS side due to fermionic excitations are explained in the SM [52].

The bound-state wave functions $v_n(x)$ of the Rydberg potential in the BCS and BEC regimes are presented in Fig. 3, see SM [52] for all bound-state wave functions u_n and v_n. Each well may host a series of bound states when the depth of the Rydberg potential is enough to compete with the pairing in the Fermi superfluid. Thus, there is a competition between the intercomponent fermion attraction to maintain the Cooper pairs and the attraction among the Rydberg atom and the fermions to form molecules. The bound-state energies in the BCS regime are clearly separated, and each bound state consists of a single fermion. This implies that the resulting diatomic Rydberg molecules originate from individual fermions due to broken Cooper pairs.

The bound states in the BEC regime shown in Fig. 3(b) are more complex. Indeed, focusing on the furthest well, the first two bound states are clearly separated in energy, indicating that they correspond to diatomic Rydberg molecules. However, the subsequent two higher vibrational bound states in the same well are energetically adjacent with almost identical wave functions. Together with the enhanced gap function shown in Fig. 2, the twin bound states suggest the presence of a locally trapped Cooper pair. Therefore, the furthest well hosts a triatomic Rydberg molecule as an excited vibrational state in the BEC regime due to the combination of the strong Cooper pairing and the Rydberg potential being capable of trapping the Cooper pair. There is also a pair of bound states with almost identical binding energies and wave functions localized in the secondary well illustrated in Fig. 3(b). These are again evident of the creation of another triatomic Rydberg molecule. Therefore, the double-well approximate Rydberg potential depicted in Fig. 1 is able to host both diatomic and triatomic Rydberg molecules. Although the excited vibrational-state wave functions may extend into the inner potential wells, a four-well calculation, described in SM [52], confirms that the results with two outermost wells are valid.

The Cooper-pair size may be estimated by the BCS coherence length [46]

$$\xi \approx \frac{\hbar v_f}{\Delta}, \tag{4}$$

where v_f is the Fermi velocity. For the system studied here, the full width at half maximum of the furthest (secondary) well is about $0.04L$ ($0.02L$). The Cooper-pair size of the selected BCS (BEC) case of Fig. 2 is $\xi/L \approx 0.06$ ($\xi/L \approx 0.003$) since $\Delta/E_f \approx 0.10$ and $k_f L \approx 35$ ($\Delta/E_f \approx 2.0$ and $k_f L \approx 36$). Hence, the Cooper pairs on the BCS side cannot be accommodated within the Rydberg-potential wells. In this context, only a fermion from a broken Cooper pair is captured, forming a diatomic molecule. In contrast, the Cooper pairs of the BEC case may fit into the Rydberg potential, which is deep enough to either break a Cooper pair or trap it to form a diatomic or a triatomic Rydberg molecule.

For a typical cold-atom cloud with density $n \approx 10^{14}$ cm^{-3} [25], $E_f \approx 10$kHz for Rb atoms, the depth of the Rydberg potential in Fig. 1 reaches the order of MHz. The pairing gap is roughly of the order of E_f as shown in Fig. 2, which can be orders of magnitude smaller than the depth of the Rydberg potential even on the BEC side. The Rydberg molecule lifetime is typically about 10-100 μs [15], while the timescale in a Fermi gas is governed by $\hbar/E_f$ (~ 0.1ms). Therefore, the above treatment of

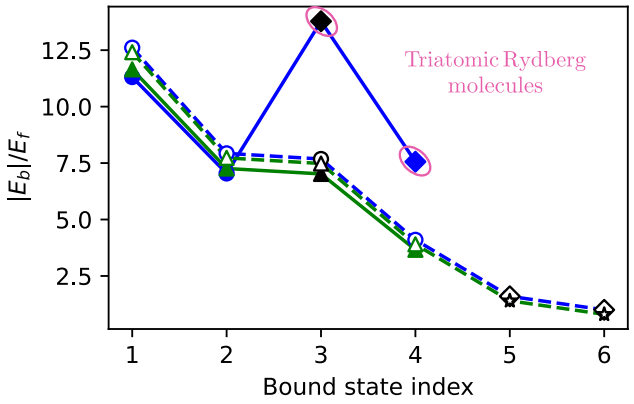


FIG. 4. Normalized binding energies from the BdG equation (circles and diamonds) and the Schrödinger equation (triangles) with the Rydberg potential of Fig. 1. Solid and hollow circles and triangles (diamonds) denote diatomic (triatomic) Rydberg molecules. Dashed (solid) lines connect the data on the BCS (BEC) side with $g = 0.7$ and $\mu = 0.20E_f$ ($g = 3.6$ and $\mu = -0.46E_f$). Blue and green (black) symbols denote the bound states in the outer (inner) well of the Rydberg potential. The higher bound states with indices $5, 6$ occupy both wells. Each triatomic Rydberg molecule binds a Cooper pair.

quasi-equilibrium of a Fermi superfluid in the presence of Rydberg molecules is physically valid. The Rydberg potential is seen as a spatially localized impurity to the Fermi superfluid, imprinting the resulting local deformation, before the global collective effects of the superfluid set in. Moreover, since there are only few Rydberg atoms in a Fermi superfluid and the Rydberg potentials are local with finite lifetime, the feedback from the Rydberg-molecule formation on the Fermi superfluid, such as heating, is assumed to be negligible. Meanwhile, a shallow Rydberg potential discussed in the SM [52] is shown to also form diatomic and triatomic Rydberg molecules.

The respective binding energies (normalized by E_f) obtained from the BdG equation with the Rydberg potential of Fig. 1 are illustrated in Fig. 4. The first two lowest-energy bound states in both BCS and BEC regimes have comparable binding energies since they correspond to diatomic Rydberg molecules consisting of the Rydberg atom and a broken-pair fermion. However, the binding energies of the higher vibrational bound states in the BCS and BEC regimes deviate more significantly because the triatomic Rydberg molecules in the BEC possess relatively larger binding energies within the trapped Cooper pairs.

We remark that the relation between the diatomic and triatomic Rydberg molecules in Fermi superfluids is more complex than that in a BEC [17] due to spin statistics and many-body effects. Indeed, adding an identical boson to a Rydberg dimer leads to a triatomic molecule with twice the diatomic binding energy. However, this does not hold for fermions due to the Pauli exclusion. Specifically, the formation of diatomic and triatomic Rydberg molecules in a Fermi superfluid competes with the binding of Cooper pairs. As such, the many-body contribution of breaking or trapping a Cooper pair plays a decisive role in creating Rydberg molecules, as it becomes apparent by the BdG calculation shown in Fig. 4.

To discern many-body from single-particle effects in the Rydberg molecule formation, we also evaluate the binding energies of diatomic Rydberg molecules with the Schrödinger equation $(h_\sigma + V_{Ryd})\psi_\sigma = E_n^S\psi_\sigma$, with h_σ from $\mathcal{H}_{BCS}$; see also SM [52] for the underlying bound states. The normalized single-particle binding energies are presented in Fig. 4. The many-body binding energies obtained from the BdG equation are in general slightly larger than the corresponding single-particle energies due to pairing effect. However, the binding energies in the BCS regime follow a similar trend with the single-particle energies, and their energy difference remains roughly constant as higher vibrational states are reached. In contrast, the BdG binding energies on the BEC side exhibit larger deviations from their single-particle counterparts. The emergence of the triatomic Rydberg molecules results in a substantial energy difference from their non-interacting counterpart due to the trapped Cooper pair which keeps its own binding energy.

Implications for experimental realization.– Spatially resolved rf spectroscopy of atomic Fermi superfluids [34, 35], following original attempts in Refs. [55, 56], maps out the local pairing gap. As described in Fig. 2, this will determine the types of Rydberg molecules since the pairing is suppressed (enhanced) in the diatomic (triatomic) Rydberg molecule. Meanwhile, the Rydberg molecules in a Fermi superfluid may serve as a probe for the Cooper-pair size because triatomic Rydberg-molecule formation is only possible when the Cooper-pair size is smaller than the width of the Rydberg potential. Differentiating the diatomic and triatomic Rydberg molecules is also achievable by Rydberg-molecule line spectroscopy [17, 19]. For example, the binding energies in the BCS (BEC) regime shown in Fig. 4 are $12.5, 7.9, 7.6, 4, 1, 1.6, 1.0$ MHz ($12, 7.7, 15, 8.4$ MHz). At those values, red detuned spectroscopy of the Rydberg lines will show peaks, corresponding to the formation of oligomeric Rydberg molecules, see for instance Fig. 2 in Ref. [17]. The Rydberg impurity-Fermi superfluid system features several tunable parameters, including the depth, width, and location of the Rydberg potential, determined by the Rydberg excitation [15, 16], and the pairing strength and particle density of the Fermi superfluid (see, e.g., Refs. [25, 46]).

Furthermore, the quasi-1D setup has several advantages. First, the many-body lifetime induced by Rydberg atoms in a lattice is found to be longer for reduced dimensions [57]. If similar enhancement also holds in the continuum, it may facilitate Rydberg-molecule formation in 1D as there are on average few fermions within the Rydberg orbit, in the cases studied here. Second, the rotational excitations of Rydberg molecules will be less relevant in 1D, significantly simplifying the bound-state

spectrum. Moreover, the 1D geometry eases i) the comparison between the Cooper-pair size and the Rydberg potential width, ii) the identification of diatomic or triatomic Rydberg molecules, and iii) the characterization of the Rydberg molecules, e.g., from the density and pairing gap profiles.

So far, the Rydberg atoms are assumed to be of different isotopes or species from the Fermi superfluid. We envision that future experiments similar to Refs. [43, 58] will prepare a boson-fermion mixture, excite the bosons to Rydberg states, produce Rydberg molecules in the Fermi superfluid, and measure the pairing gap and binding energy by spatially resolved rf spectroscopy and molecular line spectroscopy, respectively. Alternatively, if some of the fermions within the superfluid are excited into Rydberg atoms, forming homonuclear Rydberg molecules, this results in a reduced effective pairing gap, see the SM [52]. Once the excited Rydberg atoms are present, however, the corresponding bound states can be extracted through the BdG formalism. Therefore, dimer or trimer Rydberg molecules are expected via Rydberg excitations stemming from the Fermi superfluid although the reduced effective pairing gap will favor dimer Rydberg molecules.

Finally, we note that Rydberg molecules are different from Cooper-pair splitting in superconductor heterostructures [59–64] In this case, the proximity effect is utilized by dynamically sending a Cooper pair, as an excited state with spin entanglement or momentum correlation, to two separate non-superconducting regions in real space. In contrast, the fermion bound in a diatomic Rydberg molecule no longer retains the pairing correlation, while the tightly-bound Cooper pair in a triatomic Rydberg molecule localizes in real space. Along the same lines, there are subtle differences between the Rydberg molecules in Fermi superfluids and the binary tidal disruption event and pion matter. For instance, binding in binary stars (pion matter) stems from gravity (Coulomb interactions), whereas in Rydberg molecules, it is traced back to the electron-atom scattering.

Summary and outlook.– The bound states of Fermi superfluids in a Rydberg-impurity potential testify the formation of Rydberg molecules. The tunable fermion pairing gives rise to diatomic (triatomic) Rydberg molecules from broken (tightly-bound) Cooper pairs, exhibiting different features of the gap function due to their distinctive nature. The detection of the triatomic Rydberg molecules may reveal information about the Cooper-pair size, while the bound-state energies reflect pairing effects. With the rapid developments of Rydberg physics and Fermi gases, realizations of Rydberg molecules in Fermi superfluids will provide an elegant example of interfacing few- and many-body physics. Furthermore, going beyond the Leggett-BCS theory [25, 46] of the superfluid ground state, pre-formed Cooper pairs at finite temperatures correct the superfluid transition temperature and lead to the pseudo-gap effect away from the BCS regime [65, 66]. Incorporating pairing-fluctuation theories developed for homogeneous systems [27, 67–69] into the BdG formalism remains a challenge, and finite-temperature physics of Rydberg molecules awaits future research.

Acknowledgements.– C. C. C. was partly supported by the NSF (No. PHY-2310656). The authors appreciate the calculation of Rb Rydberg wave functions by Mariusz Pawlak. Support for ITAMP by the NSF is acknowledged.

[1] A. Browaeys and T. Lahaye, Many-body physics with individually controlled Rydberg atoms, Nature Physics **16**, 132 (2020).
[2] M. Saffman, T. G. Walker, and K. Mølmer, Quantum information with Rydberg atoms, Rev. Mod. Phys. **82**, 2313 (2010).
[3] C. S. Adams, J. D. Pritchard, and J. P. Shaffer, Rydberg atom quantum technologies, Journal of Physics B: Atomic, Molecular and Optical Physics **53**, 012002 (2019).
[4] X. Wu, X. Liang, Y. Tian, F. Yang, C. Chen, Y.-C. Liu, M. K. Tey, and L. You, A concise review of Rydberg atom based quantum computation and quantum simulation, Chinese Physics B **30**, 020305 (2021).
[5] D. Bluvstein, S. J. Evered, A. A. Geim, S. H. Li, H. Zhou, T. Manovitz, S. Ebadi, M. Cain, M. Kalinowski, D. Hangleiter, J. P. Bonilla Ataides, N. Maskara, I. Cong, X. Gao, P. Sales Rodriguez, T. Karolyshyn, G. Semeghini, M. J. Gullans, M. Greiner, V. Vuletić, and M. D. Lukin, Logical quantum processor based on reconfigurable atom arrays, Nature **626**, 58 (2024).
[6] X. Q. Shao, S. L. Shi-Lei Su, L. Li, R. Nath, J. H. Wu, and W. Li, Rydberg superatoms: An artificial quantum system for quantum information processing and quantum optics (2024), arXiv: 2404.05330.
[7] C. H. Greene, A. S. Dickinson, and H. R. Sadeghpour, Creation of Polar and Nonpolar Ultra-Long-Range Rydberg Molecules, Phys. Rev. Lett. **85**, 2458 (2000).
[8] M. I. Chibisov, A. A. Khuskivadze, and I. I. Fabrikant, Energies and dipole moments of long-range molecular Rydberg states, J. Phys. B: At. Mol. Opt. Phys. **35**, L193 (2002).
[9] E. L. Hamilton, C. H. Greene, and H. R. Sadeghpour, Shape-resonance-induced long-range molecular Rydberg states, J. Phys. B: At. Mol. Opt. Phys. **35**, L199 (2002).
[10] V. Bendkowsky, B. Butscher, J. Nipper, J. P. Shaffer, R. Löw, and T. Pfau, Observation of ultralong-range rydberg molecules, Nature **458**, 1005 (2009).
[11] T. Niederprüm, O. Thomas, T. Eichert, C. Lippe, J. Pérez-Ríos, C. H. Greene, and H. Ott, Observation of pendular butterfly Rydberg molecules, Nature Communications **7**, 12820 (2016).

[12] M. Althön, M. Exner, R. Blättner, and H. Ott, Exploring the vibrational series of pure trilobite Rydberg molecules, Nature Communications **14**, 8108 (2023).

[13] D. Booth, S. T. Rittenhouse, J. Yang, H. R. Sadeghpour, and J. P. Shaffer, Production of trilobite Rydberg molecule dimers with kilo-Debye permanent electric dipole moments, Science **348**, 99 (2015), https://www.science.org/doi/pdf/10.1126/science.1260722.

[14] J. D. Whalen, S. K. Kanungo, Y. Lu, S. Yoshida, J. Burgdörfer, F. B. Dunning, and T. C. Killian, Heteronuclear rydberg molecules, Phys. Rev. A **101**, 060701 (2020).

[15] J. P. Shaffer, S. T. Rittenhouse, and H. R. Sadeghpour, Ultracold Rydberg molecules, Nature Communications **9**, 1965 (2018).

[16] F. H. Christian Fey and P. Schmelcher, Ultralong-range Rydberg molecules, Molecular Physics **118**, e1679401 (2020).

[17] F. Camargo, R. Schmidt, J. D. Whalen, R. Ding, G. Woehl, S. Yoshida, J. Burgdörfer, F. B. Dunning, H. R. Sadeghpour, E. Demler, and T. C. Killian, Creation of Rydberg Polarons in a Bose Gas, Phys. Rev. Lett. **120**, 083401 (2018).

[18] R. Schmidt, H. R. Sadeghpour, and E. Demler, Mesoscopic Rydberg Impurity in an Atomic Quantum Gas, Phys. Rev. Lett. **116**, 105302 (2016).

[19] R. Schmidt, J. D. Whalen, R. Ding, F. Camargo, G. Woehl, S. Yoshida, J. Burgdörfer, F. B. Dunning, E. Demler, H. R. Sadeghpour, and T. C. Killian, Theory of excitation of Rydberg polarons in an atomic quantum gas, Phys. Rev. A **97**, 022707 (2018).

[20] J. Sous, H. R. Sadeghpour, T. C. Killian, E. Demler, and R. Schmidt, Rydberg impurity in a Fermi gas: Quantum statistics and rotational blockade, Phys. Rev. Res. **2**, 023021 (2020).

[21] A. A. T. Durst and M. T. Eiles, Phenomenology of a Rydberg impurity in an ideal Bose Einstein condensate (2024), arXiv: 2404.03980.

[22] M. Greiner, C. A. Regal, and D. S. Jin, Emergence of a molecular Bose–Einstein condensate from a Fermi gas, Nature **426**, 537 (2003).

[23] M. W. Zwierlein, C. A. Stan, C. H. Schunck, S. M. F. Raupach, A. J. Kerman, and W. Ketterle, Condensation of Pairs of Fermionic Atoms near a Feshbach Resonance, Phys. Rev. Lett. **92**, 120403 (2004).

[24] M. Bartenstein, A. Altmeyer, S. Riedl, S. Jochim, C. Chin, J. H. Denschlag, and R. Grimm, Collective Excitations of a Degenerate Gas at the BEC-BCS Crossover, Phys. Rev. Lett. **92**, 203201 (2004).

[25] C. J. Pethick and H. Smith, *Bose–Einstein Condensation in Dilute Gases*, 2nd ed. (Cambridge University Press, 2008).

[26] M. Ueda, *Fundamentals and New Frontiers of Bose-Einstein Condensation* (World Scientific, Singapore, 2010) https://www.worldscientific.com/doi/pdf/10.1142/7216.

[27] W. Zwerger, ed., *The BCS-BEC Crossover and the Unitary Fermi Gas* (Springer Berlin, Heidelberg, 2012).

[28] J. G. Hills, Hyper-velocity and tidal stars from binaries disrupted by a massive galactic black hole, Nature **331**, 687 (1988).

[29] B. C. Bromley, S. J. Kenyon, M. J. Geller, and W. R. Brown, Binary disruption by massive black holes: Hypervelocity stars, s stars, and tidal disruption events, The Astrophysical Journal Letters **749**, L42 (2012).

[30] D. Gotta, F. Amaro, D. F. Anagnostopoulos, S. Biri, D. S. Covita, H. Gorke, A. Gruber, M. Hennebach, A. Hirtl, T. Ishiwatari, P. Indelicato, T. Jensen, E.-O. L. Bigot, J. Marton, M. Nekipelov, J. M. F. dos Santos, S. Schlesser, P. Schmid, L. M. Simons, T. Strauch, M. Trassinelli, J. F. C. A. Veloso, and J. Zmeskal, Pionic hydrogen, in *Precision Physics of Simple Atoms and Molecules*, edited by S. G. Karshenboim (Springer Berlin Heidelberg, Berlin, Heidelberg, 2008) pp. 165–186.

[31] A. Hirtl, D. F. Anagnostopoulos, D. S. Covita, H. Fuhrmann, H. Gorke, D. Gotta, A. Gruber, M. Hennebach, P. Indelicato, T. S. Jensen, E.-O. L. Bigot, Y.-W. Liu, V. E. Markushin, J. Marton, M. Nekipelov, J. M. F. d. Santos, L. M. Simons, T. Strauch, M. Trassinelli, J. F. C. A. Veloso, and J. Zmeskal, Redetermination of the strong-interaction width in pionic hydrogen, The European Phys. J. A **57**, 70 (2021).

[32] T. Strauch, F. D. Amaro, D. F. Anagnostopoulos, P. Bühler, D. S. Covita, H. Gorke, D. Gotta, A. Gruber, A. Hirtl, P. Indelicato, E.-O. Le Bigot, M. Nekipelov, J. M. F. dos Santos, P. Schmid, S. Schlesser, L. M. Simons, M. Trassinelli, J. F. C. A. Veloso, and J. Zmeskal, Pionic deuterium, The European Phys. J. A **47**, 88 (2011).

[33] M. Hori, H. Aghai-Khozani, A. Sótér, A. Dax, and D. Barna, Recent results of laser spectroscopy experiments of pionic helium atoms at PSI, SciPost Phys. Proc. , 026 (2021).

[34] Y. Shin, C. H. Schunck, A. Schirotzek, and W. Ketterle, Tomographic rf spectroscopy of a trapped fermi gas at unitarity, Phys. Rev. Lett. **99**, 090403 (2007).

[35] P. A. Murthy, M. Neidig, R. Klemt, L. Bayha, I. Boettcher, T. Enss, M. Holten, G. Zürn, P. M. Preiss, and S. Jochim, High-temperature pairing in a strongly interacting two-dimensional Fermi gas, Science **359**, 452 (2018), https://www.science.org/doi/pdf/10.1126/science.aan5950.

[36] C. H. Schunck, Y.-i. Shin, A. Schirotzek, and W. Ketterle, Determination of the fermion pair size in a resonantly interacting superfluid, Nature **454**, 739 (2008).

[37] V. Bendkowsky, B. Butscher, J. Nipper, J. B. Balewski, J. P. Shaffer, R. Löw, T. Pfau, W. Li, J. Stanojevic, T. Pohl, and J. M. Rost, Rydberg Trimers and Excited Dimers Bound by Internal Quantum Reflection, Phys. Rev. Lett. **105**, 163201 (2010).

[38] I. C. H. Liu, J. Stanojevic, and J. M. Rost, Ultra-Long-Range Rydberg Trimers with a Repulsive Two-Body Interaction, Phys. Rev. Lett. **102**, 173001 (2009).

[39] J. A. Fernandez, P. Schmelcher, and R. Gonzalez-Ferez, Ultralong-range triatomic Rydberg molecules in an electric field, J. Phys. B: At. Mol. Opt. Phys. **49**, 124002 (2016).

[40] P. G. De Gennes, *Superconductivity of Metals and Alloys.*, 2nd ed., Advanced Books Classics (Chapman and Hall/CRC, Boulder, 2018).

[41] J.-X. Zhu, *Bogoliubov-de Gennes Method and Its Applications*, 1st ed., Lecture Notes in Physics, 924 (Springer International Publishing, Cham, 2016).

[42] H. Hu, L. Jiang, H. Pu, Y. Chen, and X.-J. Liu, Universal Impurity-Induced Bound State in Topological Superfluids, Phys. Rev. Lett. **110**, 020401 (2013).

[43] S. G. Crane, X. Zhao, W. Taylor, and D. J. Vieira, Trapping an isotopic mixture of fermionic ^{84}Rb and bosonic

^{87}Rb atoms, Phys. Rev. A **62**, 011402 (2000).
[44] S. Mistakidis, A. Volosniev, R. Barfknecht, T. Fogarty, T. Busch, A. Foerster, P. Schmelcher, and N. Zinner, Few-body Bose gases in low dimensions—a laboratory for quantum dynamics, Phys. Rep. **1042**, 1 (2023).
[45] M. C. Revelle, J. A. Fry, B. A. Olsen, and R. G. Hulet, 1d to 3d Crossover of a Spin-Imbalanced Fermi Gas, Phys. Rev. Lett. **117**, 235301 (2016).
[46] A. J. Leggett, *Quantum Liquids : Bose condensation and Cooper pairing in condensed-matter systems*, Oxford Graduate Texts (Oxford University Press, Oxford, UK, 2006).
[47] M. Olshanii, Atomic Scattering in the Presence of an External Confinement and a Gas of Impenetrable Bosons, Phys. Rev. Lett. **81**, 938 (1998).
[48] M. Marinescu, H. R. Sadeghpour, and A. Dalgarno, Dispersion coefficients for alkali-metal dimers, Phys. Rev. A **49**, 982 (1994).
[49] The addition of higher order terms in the Hamiltonian, including fine structure and hyperfine interactions induce electronic spin mixing (singlet and triplet) in alkali metals. However, the electronic character of the deepest potential, considered here, remains predominately triplet. Likewise, p-wave shape resonances [15, 70] in alkali atoms modify the potentials in regions closer to the core and leave unaffected the outermost potentials. For alkaline-earth Rydberg molecules, such as Sr, there is no p-wave resonance.
[50] N. Bogoliubov, On the theory of superfluidity, J. Phys. **11**, 23 (1947).
[51] B. Parajuli and C.-C. Chien, Proximity effect and spatial Kibble-Zurek mechanism in atomic Fermi gases with inhomogeneous pairing interactions, Phys. Rev. A **107**, 063314 (2023).
[52] See Supplemental Material for details on the BdG formalism, the impact of higher Rydberg excitations in the molecule formation, the effect of the Rydberg potential location, further information on the bound states, the formation of homonuclear Rydberg molecules, a comparison with the triple-well approximation, and the creation of Rydberg molecules in a noninteracting gas.
[53] C.-C. Chien, Q. Chen, Y. He, and K. Levin, Finite temperature effects in trapped Fermi gases with population imbalance, Phys. Rev. A **74**, 021602 (2006).
[54] Y. He and C.-C. Chien, Vortex structure and spectrum of an atomic Fermi superfluid in a spherical bubble trap, Phys. Rev. A **108**, 053303 (2023).
[55] J. Kinnunen, M. Rodríguez, and P. Törmä, Pairing Gap and In-Gap Excitations in Trapped Fermionic Superfluids, Science **305**, 1131 (2004), https://www.science.org/doi/pdf/10.1126/science.1100782.
[56] A. Schirotzek, Y.-i. Shin, C. H. Schunck, and W. Ketterle, Determination of the Superfluid Gap in Atomic Fermi Gases by Quasiparticle Spectroscopy, Phys. Rev. Lett. **101**, 140403 (2008).
[57] J. Zeiher, J.-y. Choi, A. Rubio-Abadal, T. Pohl, R. van Bijnen, I. Bloch, and C. Gross, Coherent Many-Body Spin Dynamics in a Long-Range Interacting Ising Chain, Phys. Rev. X **7**, 041063 (2017).
[58] R. Onofrio, Physics of our days: Cooling and thermometry of atomic fermi gases, Phys.-Usp. **59**, 1129 (2016).
[59] G. B. Lesovik, T. Martin, and G. Blatter, Electronic entanglement in the vicinity of a superconductor, The European Phys. J. B - Condensed Matter and Complex Systems **24**, 287 (2001).
[60] P. Recher, E. V. Sukhorukov, and D. Loss, Andreev tunneling, coulomb blockade, and resonant transport of nonlocal spin-entangled electrons, Phys. Rev. B **63**, 165314 (2001).
[61] L. Hofstetter, S. Csonka, J. Nygård, and C. Schönenberger, Cooper pair splitter realized in a two-quantum-dot Y-junction, Nature **461**, 960 (2009).
[62] A. Ranni, F. Brange, E. T. Mannila, C. Flindt, and V. F. Maisi, Real-time observation of Cooper pair splitting showing strong non-local correlations, Nature Communications **12**, 6358 (2021).
[63] F. Brange, R. Baruah, and C. Flindt, Adiabatic Cooper pair splitter, Phys. Rev. B **109**, L081402 (2024).
[64] J. Schindele, A. Baumgartner, and C. Schönenberger, Near-Unity Cooper Pair Splitting Efficiency, Phys. Rev. Lett. **109**, 157002 (2012).
[65] J. P. Gaebler, J. T. Stewart, T. E. Drake, D. S. Jin, A. Perali, P. Pieri, and G. C. Strinati, Observation of pseudogap behaviour in a strongly interacting Fermi gas, Nature Phys. **6**, 569 (2010).
[66] X. Li, S. Wang, X. Luo, Y.-Y. Zhou, K. Xie, H.-C. Shen, Y.-Z. Nie, Q. Chen, H. Hu, Y.-A. Chen, X.-C. Yao, and J.-W. Pan, Observation and quantification of the pseudogap in unitary fermi gases, Nature **626**, 288 (2024).
[67] K. Levin, Q. Chen, C.-C. Chien, and Y. He, Comparison of different pairing fluctuation approaches to BCS–BEC crossover, Annals of Physics **325**, 233 (2010).
[68] M. Randeria and E. Taylor, Crossover from Bardeen-Cooper-Schrieffer to Bose-Einstein Condensation and the Unitary Fermi Gas, Annual Review of Condensed Matter Physics **5**, 209 (2014).
[69] E. J. Mueller, Review of pseudogaps in strongly interacting Fermi gases, Reports on Progress in Physics **80**, 104401 (2017).
[70] M. T. Eiles, Formation of long-range rydberg molecules in two-component ultracold gases, Phys. Rev. A **98**, 042706 (2018).